Atomic Scale Fractal Dimensionality in Proteins

Duccio Medini
Immunobiological Research Institute of Siena, Chiron Vaccines, Siena, Italy

A. Widom
Physics Department, Northeastern University, Boston MA USA

(Dated: February 1, 2008)

The soft condensed matter of biological organisms exhibits atomic motions whose properties depend strongly on temperature and hydration conditions. Due to the superposition of rapidly fluctuating alternative motions at both very low temperatures (quantum effects) and very high temperatures (classical Brownian motion regime), the dimension of an atomic "path" is in reality different from unity. In the intermediate temperature regime and under environmental conditions which sustain active biological functions, the fractal dimension of the sets upon which atoms reside is an open question. Measured values of the fractal dimension of the sets on which the Hydrogen atoms reside within the Azurin protein macromolecule are reported. The distribution of proton positions was measured employing thermal neutron elastic scattering from Azurin protein targets. As the temperature was raised from low to intermediate values, a previously known and biologically relevant dynamical transition was verified for the Azurin protein only under hydrated conditions. The measured fractal dimension of the geometrical sets on which protons reside in the biologically relevant temperature regime is given by $D = 0.65 \pm 0.1$. The relationship between fractal dimensionality and biological function is qualitatively discussed.

PACS numbers: 87.14.Ee, 05.45.Df, 61.43.Hv

arXiv:cond-mat/0208184v1 8 Aug 2002

I. INTRODUCTION

There has been considerable interest in the fractal nature of atomic distributions within amorphous condensed matter[1, 2] and in particular soft condensed matter such as proteins[3, 4, 5]. Fractal sets have been studied experimentally using X-ray and small angle neutron scattering techniques which probe the correlations between different atoms within the target. Geometrical based numerical calculations [6, 7] have been used to determine the fractal dimension of secondary and tertiary structures of 90 proteins. For Azurin, the secondary structure of β-sheets and reverse-turns had the computed fractal dimension $D_1 = 1.35 \pm 0.04$. The tertiary structure of global folding had the computed fractal dimension $D_2 = 1.68 \pm 0.08$. In the above cases, coherence lengths ξ of the order of the secondary ($\xi \sim 10$Å) and the tertiary structure ($\xi \sim 40$Å) were of interest.

Rarely can the motion of an atom within biological macromolecules be described as a simple one-dimensional path. The soft condensed matter of biological organisms exhibits atomic motions whose properties depend strongly on temperature[8, 10] and hydration conditions[11, 12]. Living organisms themselves are active only within a quite limited range of temperatures and under particular environmental conditions. For very low and very high temperatures, respectively, the entropy of soft condensed biological matter is either too small (almost perfect order) or too large (severe disorder) to sustain normal biological functions. One characterization of the intermediate range of temperatures required for life employs the fractal dimension of the paths traversed by atoms within biological matter[2, 3, 13, 14, 15]. It is this intermediate range of temperature that is associated with a well known[8, 9, 10, 16] and biologically relevant[17, 18] dynamical transition from almost harmonic oscillations to strongly anharmonic modes of motion.

Ordinary paths are usually thought to be one-dimensional sets. However, at very low temperatures, quantum mechanics smears out the notion of a path; i.e. there exists quantum mechanical superposition of amplitudes of alternative paths. At sufficiently high temperatures there is superposition of Einstein-Brownian motion probabilities[2, 19]. A normal path described by a velocity v with physical units of $[cm/sec]$ is one-dimensional. A Brownian motion "path" described by a diffusion coefficient D with physical units of $[cm^2/sec]$ or area per unit time is in reality two-dimensional[19]. In the intermediate temperature range of living organisms, biomedical proton spin nuclear magnetic imaging methods exhibit an apparent diffusion coefficient (ADC) varying in time indicating fractal dimensional diffusion paths for the measured protons[20]. The fractal path dynamics of atoms will be manifest in the fractal dimensions of the spatial sets on which the atoms reside. In the intermediate temperature regime and only under environmental conditions which sustain active biological functions, the fractal dimension of these spatial sets is an open question[2, 3].

Our purpose is to present data from elastic neutron scattering off protons (hydrogen atomic nuclei) within the Azurin protein macromolecule. To our knowledge no high momentum-exchange incoherent neutron investigations have been employed to discuss the fractal nature of the proton distributions in proteins. The length scales here are truly microscopic (of order $\xi \sim 1$Å). Most importantly, none of the previous studies involves a discussion

of the temperature dependence of the fractal exponents of the proton distributions in the dynamical-transition region. In our experiments, when temperature was raised from low to intermediate values, the previously known dynamical transition[10, 16] was verified for the Azurin protein only under hydrated conditions. The resulting data substantiates that Hydrogen atomic protons reside on fractal geometrical sets of dimension $D = (0.65 \pm 0.1)$ but only in the intermediate biologically relevant temperature regimes and only in the presence of an amount of water required for biological activity.

In Sec.2, it is shown how the sets on which atoms reside may be deduced from neutron scattering data. The physical pictures which appear from such neutron data are compared with those which have been typically obtained from X-ray scattering. In Sec.3, the mathematical expression for D-dimensional fractal form factors is derived. The more conventional Debye Waller expression is shown to be a special limiting case of a fractal form factor. In Sec.4, the experimental methods for measuring the neutron elastic scattering cross section are discussed in some detail. The data is presented in Sec.5. In the concluding Sec.6, the relationships between fractal dimensionality and biological functions are qualitatively discussed.

II. SCATTERING MEASUREMENTS OF GEOMETRICAL SETS

In order to detect the geometrical sets in space within which atoms reside, it is useful to generate pictures of how the Azurin macromolecule appears to a given experimental probe. The measured fractal dimensionality of sets depends on the nature of the probe, the target and the length scale being investigated[1, 3, 21]. Two commonly used experimental diffraction probes for taking pictures of proteins are X-ray photons and thermal neutrons.

The main contribution to the elastic scattering of thermal neutrons off protein targets comes from the incoherent scattering from Hydrogen nuclei[23]. The elastic differential cross section for the neutron to scatter from N Hydrogen atom protons within the protein macromolecule is then given by[23]

$$\left(\frac{d\sigma}{d\Omega}\right)_{el} \approx \left(\frac{N\sigma_{inc}}{4\pi}\right) |F(\mathbf{Q})|^2 , \qquad (1)$$

where σ_{inc} is the single proton incoherent neutron cross section and $F(\mathbf{Q})$ is the proton form factor corresponding to a neutron momentum transfer of $\hbar\mathbf{Q} = \mathbf{p}_i - \mathbf{p}_f$. In detail, if $\rho(\mathbf{r})d^3\mathbf{r}$ denotes the probability of finding a proton (within an Hydrogen atom) at position $\mathbf{r} \in d^3\mathbf{r}$, then the form factor $F(\mathbf{Q})$ is defined as the Fourier transform

$$F(\mathbf{Q}) = \int \rho(\mathbf{r}) e^{-i\mathbf{Q}\cdot\mathbf{r}} d^3\mathbf{r}. \qquad (2)$$

Previous studies of fractal sets in proteins[13, 14, 15, 24] relied mainly on protein structure so obtained by X-ray scattering data. The cross section for such scattering with a photon wave vector transfer of $\mathbf{Q} = \mathbf{k}_i - \mathbf{k}_f$ is given by

$$\left(\frac{d\sigma}{d\Omega}\right)_{X-ray} = \frac{1}{2}\left(\frac{e^2}{mc^2}\right)^2 (1+\cos^2\Theta)\overline{|f(\mathbf{Q})|^2}, \qquad (3)$$

and the X-ray form factor is given by the Fourier transform of the density of electrons $n(\mathbf{r})$; i.e.

$$f(\mathbf{Q}) = \int n(\mathbf{r}) e^{-i\mathbf{Q}\cdot\mathbf{r}} d^3\mathbf{r}. \qquad (4)$$

The neutron scattering form factor in Eq.(2) probes the probability distribution in space $\rho(\mathbf{r})$ of the protons while the X-ray scattering form factor probes the total mean electronic density $\bar{n}$ of all the atoms and the correlations C between them; i.e.

$$\overline{n(\mathbf{r}_1)n(\mathbf{r}_2)} = \delta(\mathbf{r}_1 - \mathbf{r}_2)\bar{n}(\mathbf{r}_1) + \bar{n}(\mathbf{r}_1)\bar{n}(\mathbf{r}_2)C(\mathbf{r}_1, \mathbf{r}_2). \qquad (5)$$

The constituents of the Azurin protein as seen by X-ray photons are shown in Fig.1 using experimental results stored in the Protein Data Bank at Brookhaven National Laboratory[25]. The electronic densities of each atom are probed by X-ray diffraction. The expected picture of non-exchangeable Hydrogen atom proton positions (deduced employing chemical structures from the same X-ray data) are also shown in Fig.1. The non-exchangeable Hydrogen atom nuclei dominate the picture of the Azurin macromolecule as probed by neutron

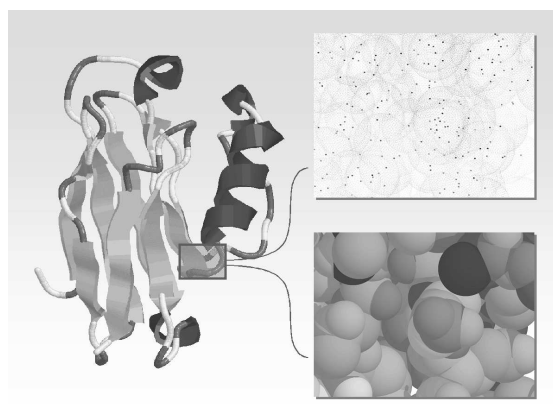

FIG. 1: Shown is the globular Azurin protein involved in electron-transfer processes. The protein structure (pdb-entry 1azu) is here pictured for the second of the four monomers in the crystalographic complex. In the magnified regions of the figure are shown (i) the expected positions of protons to be probed by thermal neutron diffraction and (ii) the electron clouds of the atoms as detected by X-ray difraction. The localized proton distributions are superimposed on the electron clouds which are less localized in space.

diffraction on atomic length scales. The electron density within an atom is represented in the picture by the empirical atomic radii[26]. The proton distributions are more localized than are the electron clouds about the nuclei.

III. FRACTAL FORM FACTORS

The usual (isotropic) Debye-Waller form factor[23]

$$F_{Debye-Waller}(\mathbf{Q}) = e^{-Q^2\overline{|\mathbf{u}|^2}/6} \tag{6}$$

corresponds to a Gaussian probability density

$$\rho_{Debye-Waller}(\mathbf{r}) = \left(\frac{3}{2\pi\overline{|\mathbf{u}|^2}}\right)^{3/2} e^{-3|\mathbf{r}|^2/2\overline{|\mathbf{u}|^2}}. \tag{7}$$

Such conventional form factors for Hydrogen atom nuclei assume harmonic oscillations in the position and are thereby valid only in the low temperature regime. For proteins at intermediate or high temperatures, one must take superpositions of Gaussian superpositions which may be employed to describe fractal form factors. How this comes about will now be discussed.

If the position of a Hydrogen atom nucleus (as a random variable) is distributed isotropically in space, then the probability for such a proton to be found within a sphere of radius R is given by

$$P(R) = 4\pi \int_0^R \rho(r) r^2 dr, \quad \text{where} \quad \lim_{R\to\infty} P(R) = 1. \tag{8}$$

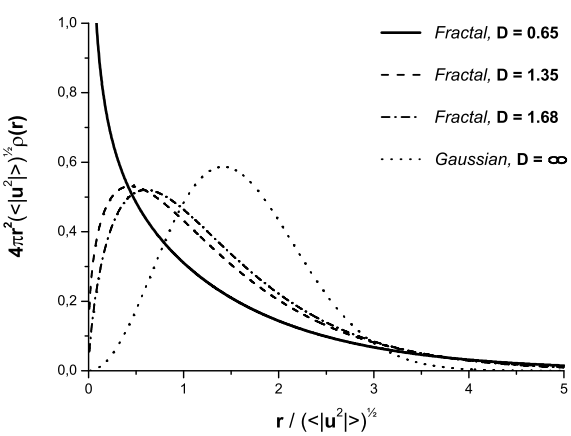

FIG. 2: Shown is a plot of $(dP(r,D)/dr) = 4\pi r^2 \rho_D(r)$ for the fractal dimensions describing (i) sets on which protons reside, (ii) secondary β-sheet structures, (iii) the tertiary folding structure and (iv) the conventional (Gaussian) Debye-Waller factor. The value of $\langle|\mathbf{u}|^2\rangle$ is fixed. Low values of D imply a strong localization of the position distribution near the equilibrium site. The long ranged tail $\rho_D(r)$ for large r inceases as D grows smaller.

The form factor in Eq.(2) may then be written

$$F(Q) = 4\pi \int_0^\infty \left(\frac{sin(Qr)}{Qr}\right) \rho(r) r^2 dr. \tag{9}$$

A probability distribution $P(R)$ will be said to exhibit a fractal dimension D if and only if

$$P(R) \sim R^D \quad \text{as} \quad R \to 0, \tag{10}$$

or equivalently if and only if

$$F(Q) \sim Q^{-D} \quad \text{as} \quad Q \to \infty. \tag{11}$$

In practise, this implies the existence of a "coherence length" ξ such that Eq.(10) holds true in the regime $R << \xi$ while Eq.(11) holds true in the regime $Q >> 1/\xi$. A simple form factor[27] incorporating both the notions of a fractal dimensionality D and a coherence length ξ may be written as

$$F_D(Q) = \left(\frac{1}{1+(Q\xi)^2}\right)^{(D/2)}. \tag{12}$$

For all (isotropic) form factor models, the mean square displacement may be computed from[23]

$$\langle|\mathbf{u}|^2\rangle = -6 \lim_{Q^2\to 0} \frac{d}{d(Q^2)} \ln F(\mathbf{Q}). \tag{13}$$

For form factor of Eq.(12), the coherence length ξ is related to the mean square displacement $<|\mathbf{u}|^2>$ via

$$\langle|\mathbf{u}|^2\rangle = 3D\xi^2. \tag{14}$$

The fractal form factor of Eq.(12) may alternatively be viewed as arising from an inhomogeneously distributed ensemble of protons each with Gaussian distributions of varying widths. The mathematical proof of this interpretation will now be exhibited. The Gamma function for $\Re e(z) > 0$ is defined as

$$\Gamma(z) = \int_0^\infty e^{-y} y^z \left(\frac{dy}{y}\right). \tag{15}$$

Change variables in the above integral using $y = as$ to obtain the identity

$$\left(\frac{1}{a}\right)^z = \frac{1}{\Gamma(z)} \int_0^\infty e^{-as} s^z \left(\frac{ds}{s}\right). \tag{16}$$

Eqs.(12) and (16) for $z = (D/2)$ and $a = 1 + (Q\xi)^2$ yield the form factor

$$F_D(Q) = \frac{1}{\Gamma(D/2)} \int_0^\infty e^{-s} e^{-sQ^2\xi^2} s^{(D/2)} \left(\frac{ds}{s}\right). \tag{17}$$

Let us now consider the density distribution due to a simple Gaussian form factor

$$\begin{aligned} \rho_G(\mathbf{r}, s) &= \int e^{-sQ^2\xi^2} e^{i\mathbf{Q}\cdot\mathbf{r}} \left(\frac{d^3\mathbf{Q}}{(2\pi)^3}\right) \\ &= \left(\frac{1}{4\pi s\xi^2}\right)^{(3/2)} e^{-|\mathbf{r}|^2/4s\xi^2}. \end{aligned} \tag{18}$$

The fractal probability density

$$\rho_D(\mathbf{r}) = \int F_D(Q) e^{i\mathbf{Q}\cdot\mathbf{r}} \left(\frac{d^3\mathbf{Q}}{(2\pi)^3} \right) \tag{19}$$

may be written as a superposition of Gaussian densities

$$\rho_D(\mathbf{r}) = \frac{1}{\Gamma(D/2)} \int_0^\infty e^{-s} s^{(D/2)} \rho_G(\mathbf{r}, s) \left(\frac{ds}{s} \right). \tag{20}$$

In detail, Eqs.(17), (18) and (19) imply that

$$\rho_D(\mathbf{r}) = \frac{1}{\Gamma(D/2)} \left(\frac{1}{4\pi\xi^2} \right)^{(3/2)} \times \int_0^\infty e^{-s} s^{(D-3)/2} e^{-|\mathbf{r}|^2/4s\xi^2} \left(\frac{ds}{s} \right). \tag{21}$$

Let us consider the probability dP that a Hydrogen atom nucleus is at a distance $r \in dr$ away from an equilibrium position; i.e. $dP(r;D) = 4\pi\rho_D(r) r^2 dr$. The Debye-Waller (Gaussian) form factor corresponds to the formally infinite value of the dimensionality $D_G = \infty$. The fractal dimensionality associated with the secondary structure of β sheets is $D_\beta \approx 1.35$ while the dimensionality associated with the tertiary structure of global folding is $D_{fold} \approx 1.68$. Finally, the value of the fractal dimension (to be discussed below) of sets on which protons reside is $D_p \approx 0.65$. The plots in Fig.2 of $dP(r;D)/dr = 4\pi r^2 \rho_D(r)$ are shown for the above important values of D. As the dimensionality D is lowered (for *fixed* $\langle |\mathbf{u}|^2 \rangle$), the distribution of particle positions are drawn inward toward the origin consistent with the definition of fractal dimensionality; i.e. $P(r;D) \sim r^D$ as $r \to 0$. The long ranged tail in $dP(r;D)/dr$ as $r \to \infty$ is increased as D grows smaller.

IV. EXPERIMENTAL METHODS

About 600 mg of Azurin powder was dehydrated under vacuum in a chamber in the presence of P_2O_5 for two days. It is known[28] for globular proteins that the ratio h of the weight of the water to the weight of the protein in the sample in the range $0.35 \leq h \leq 0.40$ corresponds to a one-shell hydration state. A portion of Azurin powder was kept dry, at an hydration level estimated as $h \leq 0,05\{\mathrm{gm}(H_2O)/\mathrm{gm}(protein)\}$. Another portion of powder was hydrated with heavy-water (D_2O). A level of $h = 0.36\{\mathrm{gm}(D_2O)/\mathrm{gm}(protein)\}$ was prepared by controlled hydration in a chamber under vacuum and in the presence of a saturated KCl heavy water solution. The water content was determined by measuring the increase in weight of the protein sample. In order to achieve an almost homogeneous hydration, the sample was arranged in the vacuum chamber to obtain the maximum exposure to the controlled environment. When the protein sample was exposed to the deuterium-hydrated environment, some of the protein protons (hydrogen) were exchanged with environmental deuterons. It is known[29] that on a reasonable time-scale only a small and definite proton-deuteron exchange takes place. To avoid an excess of proton-deuteron exchange, about one day was taken to reach the desired ratio h starting from the dry powder. After each experimental run, both the D_2O–hydrated and the dry samples were weighed again in order to verify the stability of the hydration degree throughout the experiment. In all the runs and for all the samples stability was at the level of $(\Delta h/h) \approx 0.5\%$.

Elastic neutron scattering scan were performed on the backscattering spectrometer IN13 at the Institute Laue-Langevin. An energy resolution of $\epsilon = 9\mu$eV, corresponding to an incident wavelength of 2.23 Å at a backscattering angle of 3.3^o, was achieved. The rather high incident energy of the thermal neutrons on IN13 allows an investigation of a wide range in Q^2 in the interval (0.08 $\text{Å}^{-2} < Q^2 < 25.0\text{Å}^{-2}$).

The measured quantity was the elastic part of the dynamic form factor[22],

$$S(\mathbf{Q},\omega) = \frac{1}{N} \int_{-\infty}^{\infty} \left\langle \sum_{j=1}^{N} e^{-i\mathbf{Q}\cdot\mathbf{r}_j(t)} e^{i\mathbf{Q}\cdot\mathbf{r}_j(0)} \right\rangle e^{i\omega t} \left(\frac{dt}{2\pi} \right), \tag{22}$$

where $\mathbf{r}_j(t)$ is the position of the jth Hydrogen atom nucleus at time t. In theory, the dynamic structure factor obeys the decomposition[22]

$$S(\mathbf{Q},\omega) = |F(\mathbf{Q})|^2 \delta(\omega) + S'(\mathbf{Q},\omega) \tag{23}$$

into an elastic $|F(\mathbf{Q})|^2\delta(\omega)$ and inelastic $S'(\mathbf{Q},\omega)$ part. In practise, one finds the elastic part by integrating the measured $S(\mathbf{Q},\omega)$ over a small but finite frequency bin ϖ. For our case, the bin size was $(\epsilon/e) = (\hbar\varpi/e) = 9$ μVolts so that

$$\int_{|\omega|<\varpi} S(\mathbf{Q},\omega) d\omega \approx |\mathcal{F}(\mathbf{Q})|^2 \ . \tag{24}$$

The elastic scattering was measured for 3 hours in the temperature range 20 K $< T <$ 300 K (i) at 28 temperatures for D_2O–hydrated and (ii) at 31 different temperatures for the dry powder. In both cases, about 200 mg of sample was held in a standard flat aluminum cell with internal spacing of .5 mm placed at an angle of 135° to the incident beam. The data were corrected to take into account the incident flux, cell scattering, self shielding and the detector response which refers to the sample at the lowest temperature ($T_{min} = 20$ K). An average transmission probability of 0.95 was obtained. Neither multiple scattering nor multi-phonon corrections were applied. In both the hydrated and the dry cases, the scattering intensity was largely dominated by the incoherent contribution of the protein hydrogen atoms (without proton-deuteron exchange in the hydrated sample). The coherent and other incoherent contributions are estimated at less than the 5% of the overall scattering probability.

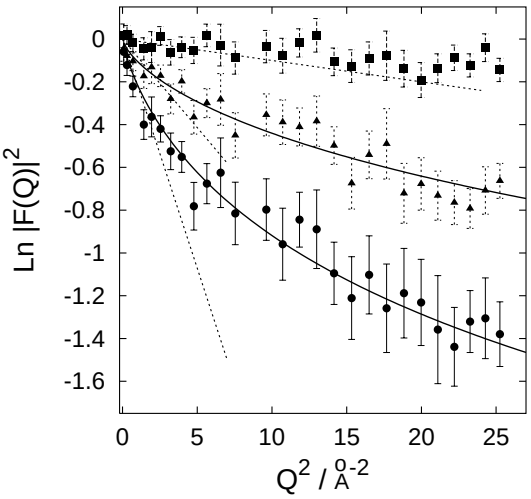

FIG. 3: The experimental squared structure factor $|F(Q)|^2$ is shown for three temperatures ($50K$, $215K$ and $295K$ from top to bottom) together with the theoretical form factor expressions (Eqs.(12) and (14) for the fractal case, and Eq.(6) for the Debye-Waller case). The solid lines are maximum likelihood fits to the fractal form factor. The dashed lines are fits to the Debye-Waller form factor using experimental values of the mean square displacement defined in Eq.(13). Experimental data from dry Azurin powder (not shown) reveal a much smaller departure from the Debye-Waller behavior.

V. ELASTIC NEUTRON SCATTERING DATA

Shown in Fig.3 are measured values of $|F(\mathbf{Q})|^2$ for the hydrated Azurin powder obtained from neutron diffraction. The experimental results may be compared with (i) the standard Debye-Waller model Eq.(6) or (ii) the structure factor Eq.(12) of a set with fractal dimensionality D. The dotted lines in Fig.3 represent the Debye-Waller form factor of Eq.(6) in terms of the mean square displacements. The mean square displacement was obtained from the data in accordance with Eq.(13). In order to achieve an experimental definition of the mathematical $Q \to 0$ limit we used a multiple fit procedure. We chose the lowest 4, 5, 6 and 7 experimental points in Q^2. For each temperature, the best fit was obtained as the reduced-χ^2 weighted average of the four possibilities employing different numbers of Q^2 values. The solid lines represent the maximum likelihood estimate of fractal dimension D employed in Eq.(12). At very low temperatures, the description of the data in terms of the Debye-Waller form factor is reasonable. For dry Azurin (data not shown), only small deviations from the Debye-Waller form factor were observed. For hydrated Azurin, as the temperature increases, very large deviations from the Debye-Waller appear in the data. In regimes wherein these large deviations were observed, a form factor of fractal dimension D provided an accurate description of the experimental results.

In order to model the distances that the Hydrogen atom protons wander from their mean equilibrium positions, we use a parametric Einstein model; i.e. the mean square displacement at temperature T is described in terms of an effective temperature dependent Hooks force constant $K(T) = m\Omega^2(T)$ where m as the proton mass.

$$\left\langle |\mathbf{u}|^2 \right\rangle_T = \left(\frac{3\hbar}{2m\Omega(T)} \right) \coth \left(\frac{\hbar\Omega(T)}{2k_B T} \right). \qquad (25)$$

If the Hydrogen atom proton were attached to an equilibrium position by a simple Hook's law spring $K_0 = m\omega_E^2$ to its equilibrium position, then a single Einstein frequency[23] ω_E would adequately fit the experimental data for $\left\langle |\mathbf{u}|^2 \right\rangle_T$. In reality, there is no single frequency ω_E for proton oscillations. Nevertheless, one may still define an effective temperature dependent frequency $\Omega(T)$ to describe the mean strength of forces restoring the Hydrogen atom to its equilibrium position. In the hydrated Azurin protein samples, we find at the lowest temperatures $\Omega(T \to 0) = \omega_E$ while at higher temperatures the restoring forces are softer and so the frequency is lower; i.e. $\Omega(T > T_{dt}) = \omega_S < \omega_E$. We have here introduced a dynamical transition temperature T_{dt} to characterize the softening of of the oscillation frequency spectrum as will now be discussed.

The powder-averaged mean square displacement data from the hydrated sample are shown in Fig.4. The

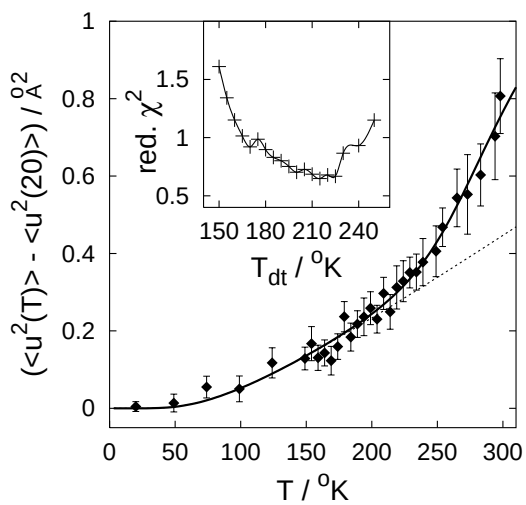

FIG. 4: The mean square Hydrogen atom displacements of the hydrated protein are obtained from a low-Q^2 analysis of $|F(Q)|^2$ as in Eq.(13). The dashed line is the best least-square fit to the Einstein model Eq.(25) with a frequency $\Omega(T) = \omega_E$ independent of temperature. The values of the reduced-χ^2 associated with such fixed frequency fits are shown in the inset as a function of T_{dt}. The minimum reduced-χ^2 is obtained for $T_{dt} = 215\ K$ which corresponds to an Einstein harmonic frequency $\omega_E/2\pi = 5.20 \pm 0.02\ THz$. In the case of the dry protein (data not shown), an Einstein model fit was possible for all temperatures with no dynamical transition. The solid curve is the best fit to the hydrated protein data with the effective frequency $\Omega(T)$ as a function of temperature.

data displays a marked temperature dependences not present in the dry Azurin sample. The marked temperature dependence has also been observed in many other types of hydrated protein samples employing many techniques [8, 9, 10, 30, 31, 32, 33, 34] including neutron diffraction [10, 11, 16, 18, 35] in the temperature range ($180\,\mathrm{K} < T_{dt} < 220\,\mathrm{K}$). The behavior of the mean square displacements as a function of temperature is independent of secondary protein structure details, and has been characterized by a dynamical transition in temperature from a harmonic to a non-harmonic regime. In order to unambiguously determine a dynamical transition temperature T_{dt}, we fit a simple single frequency Einstein model to the experimental mean square displacements for $0 < T < T_{dt}$ and then we varied the range values of T_{dt}. The reduced-$\chi(T_{dt})^2$ of these analyses was plotted as shown in the insert of Fig.4. The best reduced-χ^2 agreement with experimental data is obtained for $T_{dt} = (215 \pm 5)$ K. The dotted curve in the main of Fig.4 shows the relative theoretical fit to the data, corresponding to a frequency of $(\omega_E/2\pi) = 5.20 \pm 0.02$ THz uniform in temperature. This curve reproduces well the experimental behavior at low temperature taking quantum effects correctly into account. Above T_{dt} such a simple Einstein model is clearly inadequate for the present hydrated sample. We fit the data with a smooth Fermi function merely to extrapolate the temperature dependent $\Omega(T)$ from the low temperature value of $\Omega(T \to 0) = \omega_E$ to the higher temperature value of $\omega_S < \omega_E$. In the entire range of experimental temperatures, we have $\omega_E \geq \Omega(T) \geq \omega_S$. The frequency $\Omega(T)$ is a smoothly decreasing function of temperature. The solid curve in Fig.4 shows the parametric Einstein model fit to the experimental mean square displacement data as a function of temperature. The experimental softened frequency of the high temperature regime is given by $(\omega_S/2\pi) = 3.96 \pm 0.1$ THz. In the inset of Fig.5, we show the experimental points for the effective frequency $\Omega(T)$ as determined by the experimental mean square displacements and Eq.(25). The solid curve represents the Fermi function fit to the experimental $\Omega(T)$, the width of the transition being $\Delta T = 25 \pm 1$ K. The temperature scale is in reduced units relative to the dynamical transition temperature T_{dt}.

Our central results concerning the fractal dimensionality of the hydrated protein are shown in Fig.5. The maximum likelihood values of the fractal dimension D are plotted as function of the reduced temperature. Well above the dynamic transition temperature, where the effective restoring to equilibrium forces on the Hydrogen atom proton are softened, the fractal dimension of the set in which the proton resides is well defined and given by $D = 0.65 \pm 0.1$. As the temperature is decreased, the dimension of the set grows until (for say $D > 2$) the likelihood fits are so broad as to become meaningless. In the dry case, there is no likelihood convergence in any temperature regime. Under hydrated conditions for $T \geq 1.15\ T_{dt}$, the fractal dimension characterizes those protein samples whose parameters are neighboring the range allowing normal biological functions.

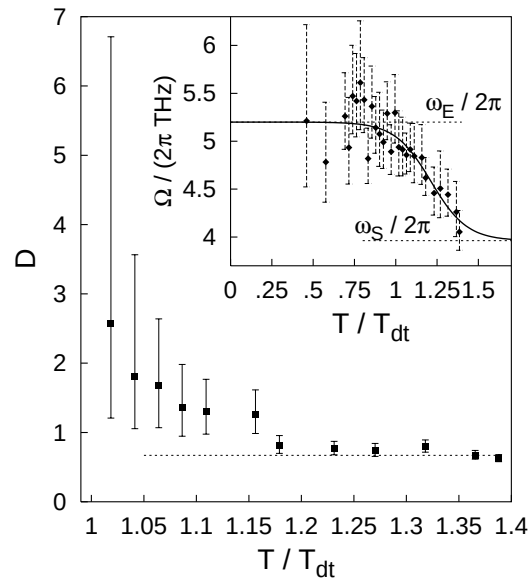

FIG. 5: Shown is the fractal dimension D obtained from the maximum likelihood fit of hydrated protein experimental $|F(Q)|^2$ data to the fractal form factor of Eqs.(12) and (14). The dashed line corresponds to the asymptotic value of $D = 0.65 \pm 0.1$. The dynamical transition temperature is $T_{dt} = 215K$. For the dry protein, likelihood convergence problems indicated that the fractal dimension D was not a useful parameter for describing the data. In the insert, diamonds give the values of $\Omega(T)/2\pi$ in Eq.(25) at each experimental temperature. The solid line is the parameterized $\Omega(T)/2\pi$ obtained by fitting the average mean-square displacements to Eq.(25). The best fit is obtained for $\omega_E/2\pi = (5.20 \pm 0.02)THz$ and $\omega_S/2\pi = (3.96 \pm 0.1)THz$.

VI. CONCLUSIONS

Some remarks on our definition of fractal dimension are in order. For the case under discussion, the fractal dimensionality D is derived from *incoherent* neutron scattering from single Hydrogen nuclei. For the atomic length-scale of these experiments, D is the fractal dimension of the set on which a single proton resides. This fractal dimension D is defined independently of the positions of the other atoms. There has been considerable previous and important work based on *coherent* scattering experiments measuring fractal sets of dimension d wherein $1.2 < d < 1.7$. Coherent scattering depends on amplitude superposition interference from pairs of different atoms. The correlation dimension d, describes sets that span a larger length scale and require the positions of atomic pairs for their definition. These larger length scales are connected with the pair-correlation properties of the α-carbons of the polypeptide chain[3, 37] or with length-scales typical of the secondary and tertiary structures. The density fractal dimension D of this work de-

scribes the length scales of inter-atomic spacing while the correlation fractal dimension d describes the length scales of the full protein size. (The length scale in diffraction experiments is $\sim Q^{-1}$.) To our knowledge no relevant temperature dependence has been observed for the correlation fractal dimension d. Only the interaction with environmental conditions related to major changes (denaturation) in the global structure[21] had any effect on the values of d. In the present case, the density fractal dimension D is only well defined when the protein sample is at biologically relevant temperatures and in the biologically relevant hydrated condition. In regimes wherein the protein is in tact but not anywhere near the form required for normal biological life functioning, D shows a strong divergence and becomes experimentally ill defined.

A principle biological function of Azurin is electron transfer. It is known that the electron-transfer efficiency of membrane protein ensembles is strongly reduced by lowering the temperature below that of the dynamical transition[17]. More recently, it has been shown [38] that protein atomic-level dynamics can amplify the electron transfer rates via the quantum interference of amplitudes from alternative paths. The regime of normal biological functions is also the regime for exhibiting atomic length scale single particle sets of fractal dimension D. What sense can be made of this observation?

A large organization (protein) functions collectively. An individual unit (atom) within the organization wanders to and fro. If the motions of individual units involve a dimensionally large set (say two or three dimensions), then the unit moves all over a neighborhood in very many random directions and taking very many possible jumps of quite indefinite lengths. If the unit moves in fewer directions and with a smaller number of possible differing length scales, then the fractal dimension D of the set on which the unit lives is also smaller. This occurs above the dynamical transition temperature wherein the time scale (Ω^{-1}) of the motion is increased. If each unit (atom) has fewer definite paths and fewer individual choices of motion, then the resulting fractal dimensional residential set is indicative of the healthy collective functioning of the larger organization (protein).

Acknowledgments

DM would like to gratefully thank Alessandro Paciaroni for his relevant help in measurements and for useful discussions; Alessandro Desideri and Maria Elena Stroppolo are kindly acknowledged for having provided the samples; the ILL is acknowledged for experimental resources; this work was partially supported with an INFM grant.

[1] J. E. Martin and A. J. Hurd, J. Appl. Cryst. **20**, 61 (1987).
[2] R. Orbach, Science **231**, 814 (1986).
[3] G. C. Wagner, J. T. Colvin, J. P. Allen and H. J. Stapleton, J. Am. Chem. Soc. **107**, 5589 (1985).
[4] J. T. Colvin and H. J. Stapleton, J. Chem. Phys **82**, 4699 (1985).
[5] R. Elber and M. Karplus, Phys. Rev. Lett. **56**, 394 (1986).
[6] C. X. Wang, Y. Y. Shi and F. H. Huang, Phys. Rev. A **41**, 7043 (1990).
[7] Y. Xiao, Phys. Rev. E **49**, 5903 (1994).
[8] F. Parak and H. Formanek, Acta Crystallogr. A **27**, 573 (1971).
[9] H. Frauenfelder, G. A. Petsko and D. Tsernoglou, Nature **280**, 558 (1979).
[10] J. C. Smith, Quar. Rev. of Biophys. **24**, 227 (1991).
[11] M. Ferrand, A. Dianoux, W. Petry and G. Zaccai, PNAS USA **90**, 9668 (1993).
[12] V. Reat, R. Dunn, M. Ferrand, J. L. Finney, R. M. Daniel and J. C. Smith, PNAS USA **97**, 9961 (2000).
[13] O. Entin-Wohlman, U. Sivan, R. Blumenfeld and Y. Meir, in: *Fractals in Physics*, edited by A. Aharony and J. Feder. Amsterdam: Elsevier Science Publishers B.V., 93 (1989).
[14] R. Elber, in: *The Fractal Approach to Heterogeneous Chemistry: Surfaces, Colloids, Polymers*, edited by D. Avnir. New York: John Wiley and Sons, 441 (1990).
[15] J. Teixeira, in: *On Growth and Form, Fractal and non-fractal patters in physics*, edited by H. E. Stanley and N. Ostrowsky, Martinus Nijhoff Publishers, Dordrecht, 145 (1986).
[16] A. Paciaroni, F. Sacchetti and S. Cannistraro, J. Chem. Phys. **261**, 39 (2000).
[17] F. Parak, E. N. Frolov, A. A. Kononenko, R. L. Mossbauer, V. I. Goldanskii and A. B. Rubin, FEBS Lett. **117**, 368 (1980).
[18] U. Lehnert, V. Reat, M. Weil, G. Zaccai and C. Pfister, Biophys. J. **90**, 9668 (1993).
[19] B. B. Mandelbrot, *The Fractal Geometry of Nature*, edited by W. H. Freeman and Co., New York (1982).
[20] A. Widom and H. J. Chen, J. Phys. A **28**, 1243 (1995).
[21] S. H. Chen, and J. Teixeira, Phys. Rev. Lett. **57**, 2583 (1986).
[22] M. Bee, *Quasielastic Neutron Scattering: Principles and Applications in Solid State Chemistry, Biology and Materials Science*, Adam Hilger, Bristol and Philadelphia (1988).
[23] S. Lovesey, *Theory of Neutron Scattering from Condensed Matter*, Oxford Science Publications, Oxford: Clarendon (1984).
[24] M. Lewis and D. C. Rees, Science **230**, 1163 (1985).
[25] H. Nar, A. Messerschmidt, R. Huber, M. Van de Kamp and G. W. Canters, J. Mol. Biol. **221**, 765 (1991).
[26] J. C. Slater, J. Chem. Phys. **39**, 3199 (1964).
[27] M.E. Fisher and R. J. Burford, Phys. Rev. **156**, 583 (1967).
[28] *Protein-solvent Interactions* edited by R. B. Gregory and

M. Dekker, New York (1995).
[29] M. Settles and W. Doster, Farad. Disc., 103 (1996).
[30] H. Keller and P. G. Debrunner, Phys. Rev. Lett. **45**, 67 (1980).
[31] F. Parak, E. N. Frolov, R. L. Mossbauer and V. I. Goldanskii, J. Mol. Biol. **145**, 825 (1981).
[32] S. G. Cohen, E. R. Bauminger, L. Nowik, S. Ofer and J. W. Yariv, Phys. Rev. Lett. **46**, 1244 (1981).
[33] E. W. Knapp, S. F. Fisher and F. Parak, J. Phys. Chem. **86**, 5042 (1982).
[34] B. F. Rasmussen, A. M. Stock, D. Ringe and G. A. Petsko, Nature **357**, 423 (1992).
[35] W. Doster, S. Cusack and W. Petry, Nature **337**, 754 (1989).
[36] J. Fitter, R. E. Lechner and N. A. Dencher, Biophys. J. **73**, 2126 (1997).
[37] J. A. McCammon, Rep. Prog. Phys. **47**, 1 (1984).
[38] I. A. Balabin and J. N. Onuchic, Science **290**, 114 (2000).